LBL-35946
UC-600

Lawrence Berkeley Laboratory
UNIVERSITY OF CALIFORNIA

EARTH SCIENCES DIVISION

Presented at the Symposium on the Non-Proliferation Experiment Results and Implications, Rockville, MD, April 18–21, 1994, and to be published in the Proceedings

Recording Experiment on Rainier Mesa in Conjunction with a Reflection Survey

L.R. Johnson

June 1994

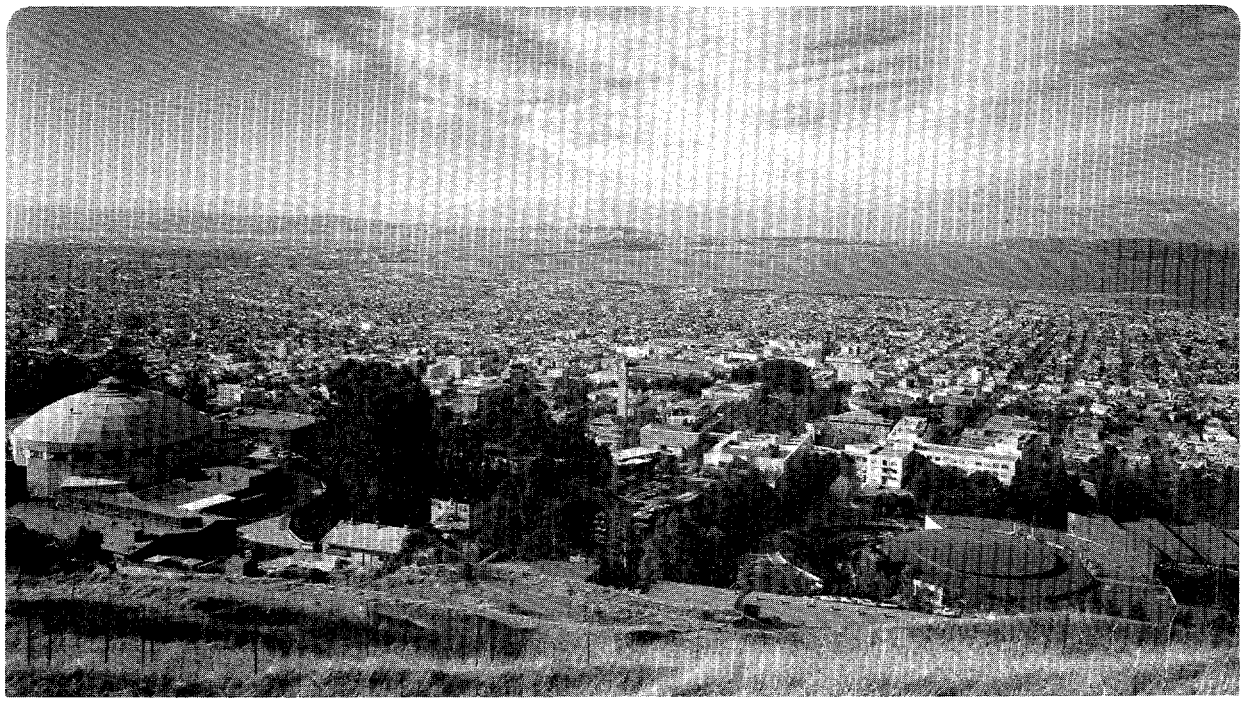

Prepared for the U.S. Department of Energy under Contract Number DE-AC03-76SF00098

DISCLAIMER

Portions of this document may be illegible in electronic image products. Images are produced from the best available original document.

LBL-35946
UC-600

Recording Experiment on Rainier Mesa in Conjunction with a Reflection Survey

Lane R. Johnson

Center for Computational Seismology
Earth Sciences Division
Lawrence Berkeley Laboratory
University of California
Berkeley, California 94720

June 1994

This work was supported by the Air Force Office of Scientific Research under Contract No. F49620-94-1-0197 and also by the Director, Office of Energy Research, Office of Basic Sciences, Earth Sciences Division, of the U.S. Department of Energy under Contract No. DE-AC03-76SF00098.

Recording Experiment on Rainier Mesa in Conjunction with a Reflection Survey

Lane R. Johnson
Center for Computational Seismology, Lawrence Berkeley Laboratory
Department of Geology and Geophysics, University of California
Berkeley, California 94720

Abstract

The chemical explosion of the NPE was recorded on the surface of Rainier Mesa along the same line which had previously been the site of a high resolution reflection survey. Six three-component accelerometer stations where distributed along the 550 meter line, which was offset about 600 meters from the epicenter of the explosion. The bandwidth of the acceleration data extends to 100 Hz. Even though the separations of the stations was only about 100 meters, the waveforms and the amplitudes exhibited considerable variability, especially for the transverse component of motion. The maximum accelerations ranged between 0.27 g and 1.46 g, with the maximums of the average traces being 0.57 g on the radial component, 0.28 on the transverse component, and 0.50 g on the vertical component. Using the results of the reflection survey to help constrain the velocity model, the acceleration data were inverted to obtain a preliminary estimate of the seismic moment tensor of the NPE. This result is a strong diagnostic for the NPE being an explosion, showing a somewhat asymmetric extensional source with very small shear components. When interpreted in terms of a spectral model and scaling relationships, the isotropic moment tensor indicates a yield of 1.4 kt, an elastic radius of 116 meters and a cavity radius of 15.5 meters. This interpretation includes a source time function which contains appreciable overshoot, and, if shown to be reliable, this feature of the explosion could have a significant effect upon the analyses of other types of seismic data.

Introduction

The waveforms recorded on seismograms represent the combined effects of the seismic source and wave propagation through the material intervening between the source and receiver sites. All verification methods that use seismic data must first deal with these wave propagation effects, as these essentially have to be removed in order to isolate the information on the seismogram which is useful in making inferences about properties of the seismic source. Success in the task of verifying explosion sources is directly related to the proficiency in removing these propagation effects.

One of the standard methods of studying seismic sources is known as *moment tensor inversion.* With this approach the seismogram is shown to be a convolution between the seismic source, described as a second order *seismic moment tensor,* and a Green function which contains the propagation effects. The Green function can be obtained by solving the elastodynamic equations of motion in an earth

model which is representative of the geological structure in the region where the source and receivers are located. This representation of the problem is linear so that standard inverse methods can be used to extract an estimate of the seismic source from the waveform data contained on the seismograms. With this approach all propagation effects are contained in the Green functions and so the reliability of the results is directly related to the accuracy of these functions, which is in turn related to the fidelity between the earth model and the actual earth structure. Thus it would appear that the availability of an accurate estimate of earth structure would be a critical requirement for the success of the moment tensor inversion method.

The NPE provided an excellent opportunity to check seismic methods of estimating explosion properties in general, including the method of moment tensor inversion. In order to check the dependence of this method on the model assumed for the earth structure, an attempt was made to obtain a fairly detailed estimate of the velocity structure in the vicinity of the experiment. Prior to the NPE a surface reflection profile was obtained along a north-south line on the surface of Rainier Mesa slightly to the west of the epicenter (Majer et al., 1994). The data from this profile were processed to obtain an estimate of the velocity and density structure of Ranier Mesa in the vicinity of the NPE. At the time of the NPE this surface reflection profile was reoccupied with seismographs. Thus the data recorded by these seismographs can be subjected to the moment tensor inversion method using the velocity model which had been obtained specifically for this region. This would appear to be an optimum situation for moment tensor inversion, and thus the results should allow a critical evaluation of the capabilities of this method. The primary objective of the present study is to apply the moment tensor inversion method to the data recorded from the NPE and evaluate the results.

Experiment Parameters

The shot information for the NPE which was used in this study is as follows:

origin time = 00h 01m 0.080s
latitude = 37.20193 degrees N
longitude = 116.20986 degrees W
elevation = 1852.6 meters
depth = 389 meters

The explosion was recorded at six sites distributed on the surface of the Rainier Mesa along the profile which had previously been occupied for the reflection study. The geometrical relationship between the recording sites and the NPE is shown in Figure 1. The six recording sites were located along a roughly north-south line about 550 meters in length and located about 600 meters west of the NPE epicenter. The slant distances to the recording sites from the NPE shot point ranged between 709 and 853 meters. Details of the recording locations are given in Table 1.

The seismographs were accelerometers (FBA-23 models) with nominal natural frequencies of either 50 or 100 Hz. Each station had three components oriented in north, east, and vertical directions. The data were digitally recorded at 24 bit resolution and a sampling interval of 0.004 sec. Timing was by an internal clock which was synchronized to satellite time.

Waveform Data

All of the recording units operated successfully with 100% data recovery. For the purposes of display, the horizontal records were rotated into radial and transverse components using the azimuths listed in Table 1. The recorded data are shown in Figures 2, 3, and 4. First motions are always in the same direction on the vertical and radial components, up and away from the source, but have variable directions on the transverse components. The maximum accelerations at all stations are listed in Table 2. The maximum accelerations ranged between 0.27 g and 1.46 g with considerable variation between near-by stations. The maximum acceleration appears on either the vertical or radial component with the maximum on the transverse component always being the smallest, averaging about 55% the mean of the other two components.

The six recording stations of this experiment span a rather limited range in distance and azimuth from the NPE, and thus only a small fraction of the focal sphere has been sampled by the direct waves which arrive at these stations. In spite of this and the fact that the separation between adjacent stations was only about 100 meters, the waveforms and amplitudes exhibit considerable variability. While the polarity of first motions and general waveforms on the vertical and radial show a general similarity between stations, there are some later arriving pulses which have high frequencies, large amplitudes, and significant differences between the stations. The variability on the transverse components is quite pronounced. Few of the waveforms correlate between adjacent stations and even the polarity of first motions is not consistent across the profile.

After time shifting to line up the first motions on the records, the seismograms at the six stations were averaged for each of the components separately to arrive at the traces shown in Figure 5. Note that the maximum accelerations on the average traces are less than the maximum accelerations on almost all of the stations (compare with Table 2), suggesting that the sharp peaks that are causing the maximum accelerations at the individual stations are not coherent between the stations. In general the average traces have the appearance of having less high frequency energy than the individual traces for the vertical and radial components, but not on the transverse component.

First Arrival Times

With the origin time of the NPE known and absolute timing at the recording stations, it was possible to measure the time of first arriving energy at each station and then calculate the travel-time. These travel times are listed in Table 3 along with an apparent average velocity, which was obtained by dividing the slant distance by the travel time. These apparent velocities are rather slow, generally less than 2.0 km/sec. Also apparent in Table 3 is the fact that there is a systematic change in the apparent average velocity along the profile, with the north end generally being slower than the south end. This could be caused by either a lateral gradient in the average velocity of Rainier Mesa in the upper 400 meters or by a lateral change in delays in low velocity material in the upper few meters of Rainier Mesa.

Velocity Model

As mentioned in the introduction, an earlier part of this experiment had included a reflection survey on the surface of Rainier Mesa along the same profile where the recording stations were located. The velocity profile produced by the interpretation of these reflection data was thus available for the

interpretation of the waveform data recorded from the NPE. The initial analysis of the data has used a one-dimensional model of the structure, with material properties varying only in the vertical direction. This model is shown in Figure 6. Only the P velocity of this model was derived from the reflection data, and considerable use of the geological information obtained from drill holes (Baldwin et al., 1994) was used in the interpretation. That is, where the reflection data provided evidence of an increase or decrease of P velocity in a particular depth range, the model depth was adjusted to be in general agreement with the changes in lithology suggest by the logging information from the drill holes. The P velocity model was also constrained to agree with the travel times of first arrivals given in Table 3, which is essentially an apparent average velocity of 2.0 km/sec between the NPE and the recording profile. The S velocity and density were then derived from the P velocity using ratios consistent with measurements of velocity and density obtained from the drill holes. The net result is a one-dimensional model which is generally consistent with the reflection data, the geological data, and the first arrival times from the NPE.

The general features of the velocity model include rather low velocities in the weathered layer at the surface but these increase rapidly in the caprock of the mesa, the Rainier Mesa Tuff. There appears to be a decrease in velocity part way through this unit (depth of 80 meters) and a further decrease at its bottom. The underlying unit, the Paintbrush tuff, has very low velocities, but the velocities increase before reaching the depth of the NPE (389 meters) in the Tunnel Beds Units. Below the explosion depth there is a further increase in the velocity and then the Paleozoic basement is encountered at a depth of about 775 meters. In this model the material properties at the depth of the NPE are

P velocity = 2.6 km/sec
S velocity = 1.2 km/sec
density = 1.9 gm/cc

Moment Tensor Solution

The waveform data recorded by this experiment were subjected to the standard moment tensor inversion method (Stump and Johnson, 1977). All three components from the six stations were used in the inversion, for a total of eighteen seismograms, and the first 8.1 sec of data were included from each seismogram. Estimates for the six independent elements of the force moment tensor are shown in the time domain in Figure 7. It is clear that the moment tensor is dominated by its diagonal elements, as one would expect for a simple explosion. There is a slight asymmetry in these diagonal elements, the 33 term being larger than the 11 and 22 components. This same effect has been observed for other explosions at NTS and suggests that the explosion expands more in the vertical direction than in the horizontal direction, but the exact cause of this effect is not understood.

The *isotropic moment tensor* (average of the three diagonal elements) was taken as the symmetric part of the seismic source and subjected to further analysis. The modulus of the time derivative of this isotropic moment tensor is shown in the frequency domain in Figure 8. Comparing this modulus to the estimated uncertainty, there appears to be a good signal-to-noise ratio in the range between about 0.4 and 60 Hz. Within this range there is a slight increase in the modulus with increasing frequency up to a corner frequency at about 3 Hz, although the data show considerable variation in this low frequency range. Beyond the corner frequency the modulus shows a steady decrease with increasing frequency until the noise floor is reached.

The interpretation of the spectrum of the isotropic moment tensor if facilitated by parameterizing it in terms of a spectral model. In the present study the spectral model was

$$|M(f)|^2 = \frac{P_1^2}{1 + 2(2P_4^2 - 1)(f/P_2)^{P_3} + (f/P_2)^{2P_3}} + P_5$$

where

P_1 is the low frequency level, or scalar moment
P_2 is the corner frequency
P_3 is the high frequency decay rate
P_4 is the damping parameter (1 for critical damping)
P_5 is the variance of the signal independent white noise

This model was fit to the observed spectral modulus by a maximum likelihood procedure using an algorithm developed by Ihaka (1985). The dotted line in Figure 8 was obtained with this procedure with the damping constrained to have a critical value ($P_4 = 1.0$). Critical damping means that there is no peaking in the frequency domain and no overshoot in the time domain. With this type of model the estimated parameters are

- spectral parameters - without overshoot

scalar moment	57 $10^{13} N\ m$
corner frequency	2.9 *Hz*
damping	1.0
high-frequency decay	3.0

It is clear in Figure 8 that the parametric fit without overshoot does not do a good job of representing the spectrum at frequencies less than the corner frequency. Thus another fit was performed in which the damping was unconstrained and this produced the results shown in Figure 9. The estimated parameters in this case are

- spectral parameters - with overshoot

scalar moment	20 $10^{13} N\ m$
corner frequency	3.3 *Hz*
damping	0.09
high-frequency decay	2.6

This fit is considerably better at low frequencies, suggesting that a model with damping considerably less than critical is appropriate for the estimated isotropic moment tensor. Note that the two fits to the spectrum differ primarily in their values for the scalar moment, which is more than 2.5 times smaller for the case with overshoot.

Scaling Relationships

The spectral parameters estimated for the isotropic moment tensor of the NPE were converted to source properties using the scaling relationships of Denny and Johnson (1991). The working point properties which were used in these calculations were as follows:

P velocity	$\alpha = 2.6\ km/sec$
S velocity	$\beta = 1.2\ km/sec$
density	$\rho = 1.9\ gm/cc$
pressure	$P_o = 7.2\ MPa$
gas porosity	$GP = 1\%$

Then the relationship between the yield W and scalar moment M_o is given by

$$W = 294\ 10^{-12}\ \beta^{1.1544}\ P_o^{0.4385}\ 10^{0.0344GP}\ \frac{M_o}{4\pi\rho\alpha^2}$$

Using the scalar moment estimated above for the case where overshoot is included, the estimated yield for the NPE is

$$W = 1.4\ kt$$

which is about 30% greater than the announced yield for this event. The scalar moment can also be converted to the static reduced displacement potential Ψ_∞ through the relation

$$\Psi_\infty = \frac{M_o}{4\pi\rho\alpha^2}$$

which yields in the present case

$$\Psi_\infty = 1240\ m^3$$

The relationship between the elastic radius R_s and the corner frequency f_c is given by

$$R_s = \frac{\beta}{\pi f_c}$$

Again using the parameters estimated for the case with overshoot, the result is

$$R_s = 116\ m$$

This can be converted to the cavity radius R_c using the scaling relationship

$$R_c = \frac{9443}{(\rho\beta^2)^{0.7245}\ P_o^{-0.2897}}\ R_s$$

which yields

$$R_c = 15.5\ m$$

Summarizing the results for the case where overshoot is allowed in the parametric model of the moment tensor, the estimates for the NPE are as follows:

scalar moment	$M_o = 20\ 10^{13} N\ m$
static RDP	$\Psi_\infty = 1240\ m^3$
yield	$W = 1.4\ kt$
elastic radius	$R_s = 116\ m$
cavity radius	$R_c = 15.5\ m$

If these calculations are repeated with the fit to the isotropic moment spectrum that does not have overshoot, the results are:

scalar moment	$M_o = 57\ 10^{13} N\ m$
static RDP	$\Psi_\infty = 3530\ m^3$
yield	$W = 4.1\ kt$
elastic radius	$R_s = 132\ m$
cavity radius	$R_c = 17.6\ m$

It is clear that inclusion or exclusion of overshoot in the spectral model can have a significant effect upon the estimated yield.

Discussion and Summary

The present study was only a preliminary interpretation of one of the seismic experiments which was performed in the local distance range. It was rather limited in the amount of seismic data which were used and the fraction of the focal sphere which was sampled. However, it did have the advantage of being coordinated with a companion study specifically designed to determine the velocity structure which is required in the interpretation of the waveform data. It was possible to make estimates of several properties of the NPE explosion, including its yield, its physical dimension, and the amount of overshoot in its time function. Of course, the validity of these estimates can only be determined by comparing them with the other results that were obtained for the NPE.

In this preliminary interpretation of the data, only a one-dimensional velocity model was used. The variation in travel times of first arrivals, however, indicates that there are some definite three-dimensional effects which should be investigated. It is not clear whether these are systematic variations that involve the upper few hundred meters of the mesa or just local effects that involve the upper few meters under each seismographic station. The fact that some of the high frequency acceleration pulses on the seismograms do not correlate well between adjacent stations suggests that some of these local effects are present. Further study is necessary in order to explore the sensitivity of the results to the details of the velocity model used in the inversion.

The interpretation of the spectrum of the moment tensor in terms of properties of the explosion source requires reliable estimates of frequencies below the corner frequency. In this case where the size of the explosion is actually quite small, the quality of these low frequency estimates is still rather marginal. The spectrum appears to be reliable above about 0.4 Hz, based on the signal-to-noise ratio, but there is considerable scatter in this range. Thus there is considerable uncertainty in extrapolating these values to zero frequency where the scalar seismic moment is defined, and this uncertainty translates directly into uncertainty in the estimated yield of the explosion.

The results of this study indicate that significant overshoot existed in the source time function of the NPE. This is suggested by the peaking in the spectrum of the isotropic moment tensor in the vicinity of the corner frequency and the fact that parameterized fits to the spectrum are better when overshoot is included. Further study to definitely establish the presence of this overshoot are warranted because it has several ramifications. If present, it implies that the spectral shape below the corner frequency is not flat, and thus various seismic methods that use different frequencies in this range to estimate the yield of the explosion will yield different results. In the present study it was found that including the effect of the overshoot changed the estimate of the yield of the NPE by almost a factor of 3.

The interpretation of the data collected in this experiment indicates a yield of 1.4 kt for the NPE, which is about 30% greater than the actual yield. It is important to understand the reason for this difference. First, it should be pointed out that most of the other seismic methods which have been applied to the NPE also overestimated the yield, so this discrepancy is not confined to the moment tensor inversion method. One possibility relates to the fact that the scaling relationships used to convert seismic measurements to yield are based primarily upon empirical data from nuclear explosions, and it is possible that different scaling relationships are required for chemical explosions. The study of Denny and Johnson (1991), which was used for the scaling relationships in the calculations of the present study, did include both chemical and nuclear explosions, but it contained very little data, either chemical or nuclear, on yield versus moment in the range around 1 kt. Thus this question of the difference between nuclear and chemical explosions still does not have a satisfactory answer.

The results presented in this preliminary study are incomplete in that uncertainties in the estimated values have not been given, a deficiency which will hopefully be corrected by further analysis. Part of this problem is straightforward, as formal uncertainty analysis has already been included in the fitting of spectral models and the use of the scaling relationships, so carrying such uncertainties through to the final estimates is possible. It should also be possible to place uncertainty bounds upon the material properties at the working point which were used in the calculations. However, there are other parts of the uncertainty issue which are more difficult to analyze. These involve such matters as the uncertainty in the velocity model and various assumptions which were used in the inversion process. It appears that such effects will have to be investigated by repeating the analysis for a number of different sets of models and assumptions and in this way determine their effects upon the final estimates. While this is not a completely satisfactory approach from the viewpoint of a formal uncertainty analysis, it is better than ignoring such effects altogether.

Acknowledgements

The assistance of Don Lippert and Russell Sell in the field operations of this experiment is gratefully acknowledged.

References

Baldwin, M. J., R. P. Bradford, S. P. Hopkins, D. R. Townsend, and B. L. Harris-West, Geologic characteristics of the NPE site in the U12n.25 drift of N-tunnel, Nevada Test Site, in Proceedings of the Symposium on the Non-Proliferation Experiment Results and Implications, M. D. Denny et al. (eds), Lawrence Livermore National Laboratory, Livermore, CA, CONF-9404100, 1994.

Denny, M. D., and L. R. Johnson, The explosion seismic source function: models and scaling laws reviewed, in Explosion Source Phenomenology, Geophys. Monograph 65, American Geophysical Union, Washington, D.C., 1991.

Ihaka, R., Ph.D. Dissertation, University of California, Berkeley, 1985.

Johnson, L. R., Seismic source parameters, in Proceedings of the Symposium on the Non-Proliferation Experiment Results and Implications, M. D. Denny et al. (eds), Lawrence Livermore National Laboratory, Livermore, CA, CONF-9404100, 1994.

Majer, E. L., L. R. Johnson, E. K. Karageorgi, and J. E. Peterson, High-resolution seismic imaging of Rainier Mesa using surface reflection and surface-to-tunnel tomography, in Proceedings of the

Symposium on the Non-Proliferation Experiment Results and Implications, M. D. Denny et al. (eds), Lawrence Livermore National Laboratory, Livermore, CA, CONF-9404100, 1994.

Stump, B. W., and L. R. Johnson, The determination of source properties by the linear inversion of seismograms, Bull. Seismol. Soc. Am., 67, 1489-1502, 1977.

Table 1. Locations of Seismic Recording Stations

Station	Latitude deg N	longitude deg W	Elevation m	Range m	Azimuth deg
UCB100	37.20364	116.21800	2242	747	285
UCB120	37.20287	116.21716	2237	656	279
UCB140	37.20196	116.21661	2235	599	270
UCB160	37.20086	116.21667	2236	616	259
UCB180	37.19987	116.21689	2237	668	249
UCB200	37.19874	116.21746	2239	762	242

Table 2. Maximum Accelerations from Event NPE

Station	Azimuth deg	Range m	Distance m	max R cm/s**2	max T cm/s**2	max Z cm/s**2
UCB100	285	747	841	420	346	642
UCB120	279	656	759	790	463	661
UCB140	270	599	709	1310	706	1436
UCB160	259	616	724	615	266	714
UCB180	249	668	769	944	607	1053
UCB200	242	762	853	809	351	595

Table 3. Travel Times from Event NPE

Station	Azimuth deg	Range m	Distance m	Travel Time sec	Mean Vel. km/sec
UCB100	285	747	841	0.476	1.77
UCB120	279	656	759	0.432	1.76
UCB140	270	599	709	0.393	1.80
UCB160	259	616	724	0.363	1.99
UCB180	249	668	769	0.381	2.01
UCB200	242	762	853	0.402	2.12

Figure Captions

Figure 1. Geometry of the six recording sites and their relationship to the location of the NPE.

Figure 2. The radial accelerations recorded from the NPE with up motion on the seismograms indicating motion of the ground away from the source. Also shown at the bottom is the average of the six radial components. All seismograms are to the same scale, which is shown on the right where 1 g = 9.8 m/s.

Figure 3. The transverse accelerations recorded from the NPE with up motion on the seismograms indicating motion of the ground clockwise around the source as viewed from above. Also shown at the bottom is the average of the six transverse components. All seismograms are to the same scale, which is shown on the right where 1 g = 9.8 m/s.

Figure 4. The vertical accelerations recorded from the NPE with up motion on the seismograms indicating upward motion of the ground. Also shown at the bottom is the average of the six vertical components. All seismograms are to the same scale, which is shown on the right where 1 g = 9.8 m/s.

Figure 5. The average of the accelerations at the six stations for each component of motion. Time shifts to line up the first motions on the records were applied before the averages were calculated.

Figure 6. Velocity and density model for the upper part of Rainier Mesa in the vicinity of the NPE.

Figure 7. Estimates of the force moment tensor for the NPE. The directions are chosen so that 1 is north, 2 is east, and 3 is down. The maximum on the 33 component has a value of 160 10^{20} dyne cm.

Figure 8. The modulus of the Fourier transform of the isotropic moment rate tensor (solid line). The dashed line is an estimate of the uncertainty in the estimate and the dotted line is a parametric model which was fit to the modulus.

Figure 9. Similar to Figure 8 except that the parametric model fit to the modulus (dotted line) includes a damping parameter.

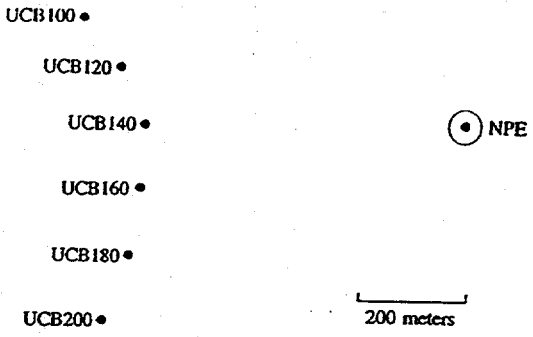
UCB100
UCB120
UCB140
UCB160
UCB180
UCB200
NPE
200 meters

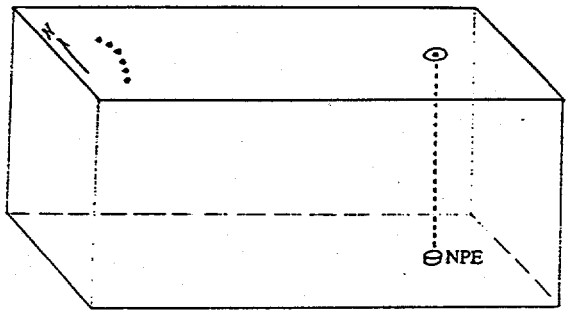
N
NPE

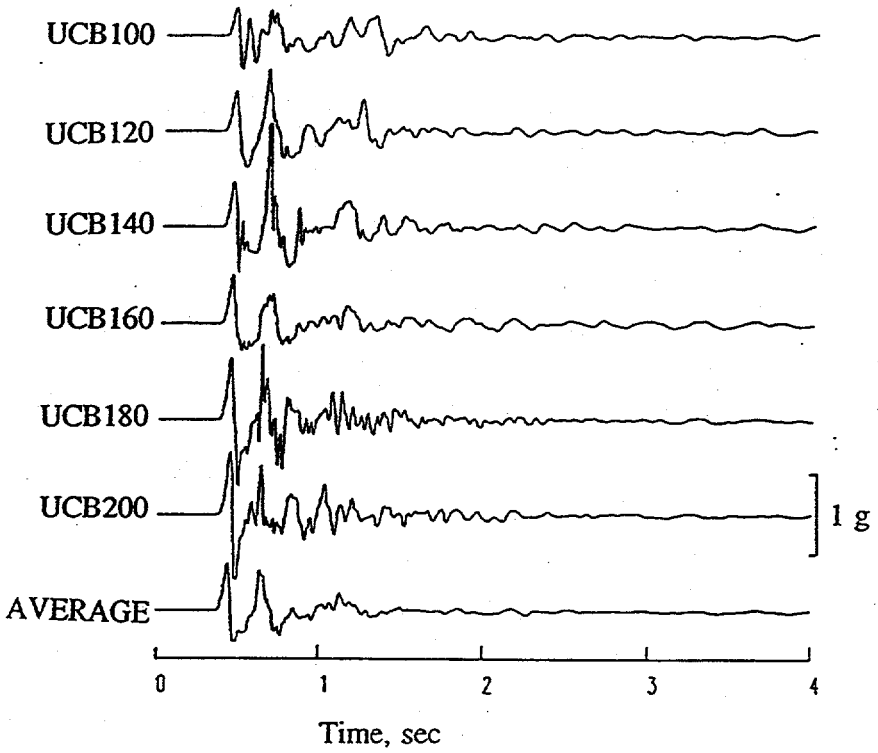
UCB100
UCB120
UCB140
UCB160
UCB180
UCB200
AVERAGE
1 g
0
1
2
3
4
Time, sec

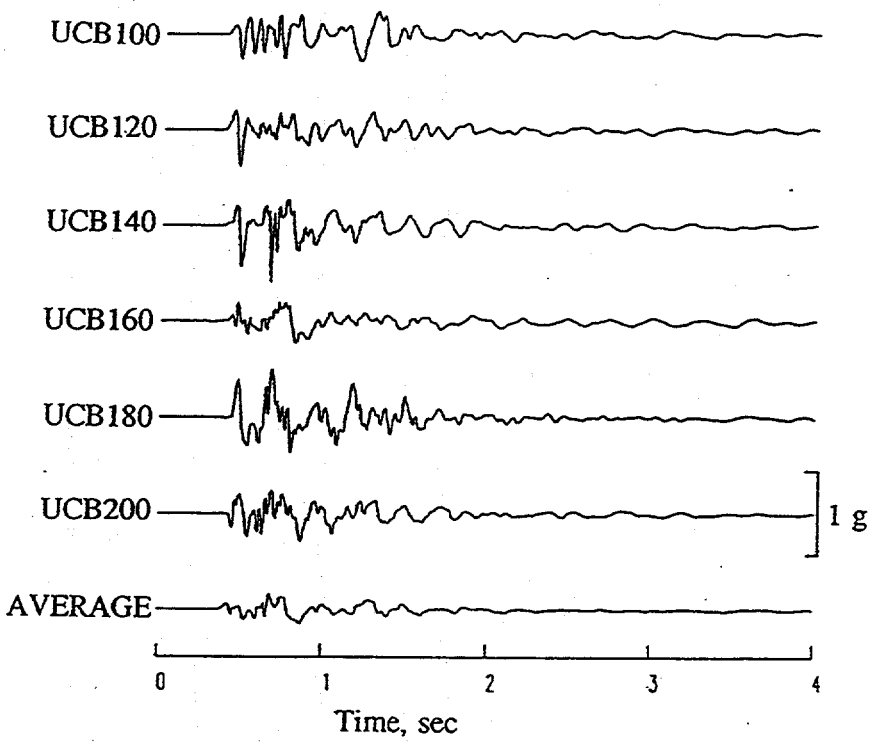
UCB100
UCB120
UCB140
UCB160
UCB180
UCB200
1 g
AVERAGE
0
1
2
3
4
Time, sec

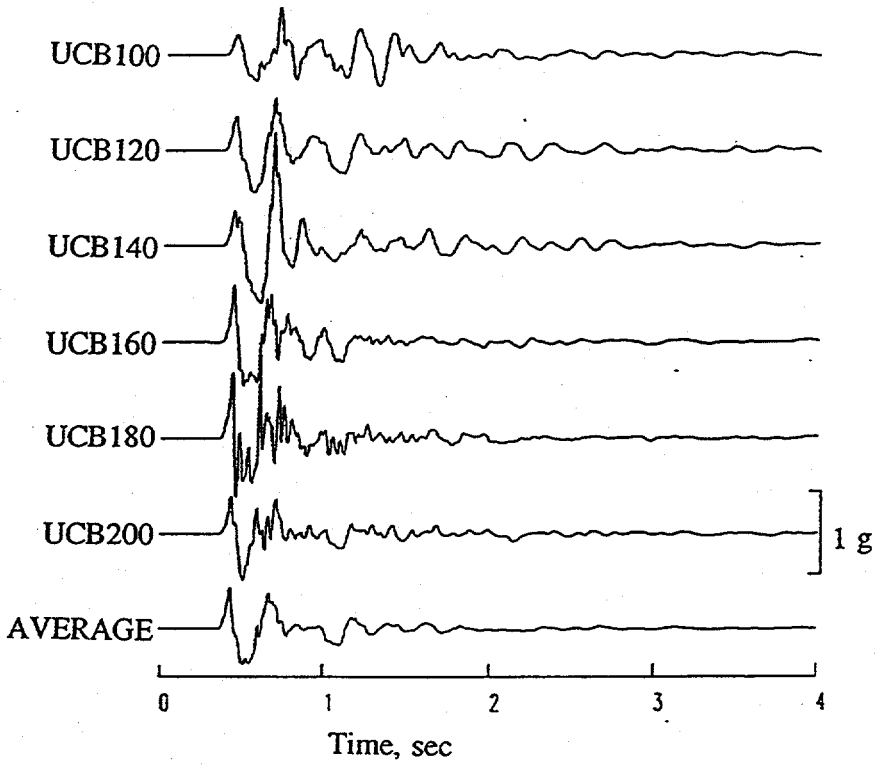
UCB100
UCB120
UCB140
UCB160
UCB180
UCB200
AVERAGE
1 g
0
1
2
3
4
Time, sec

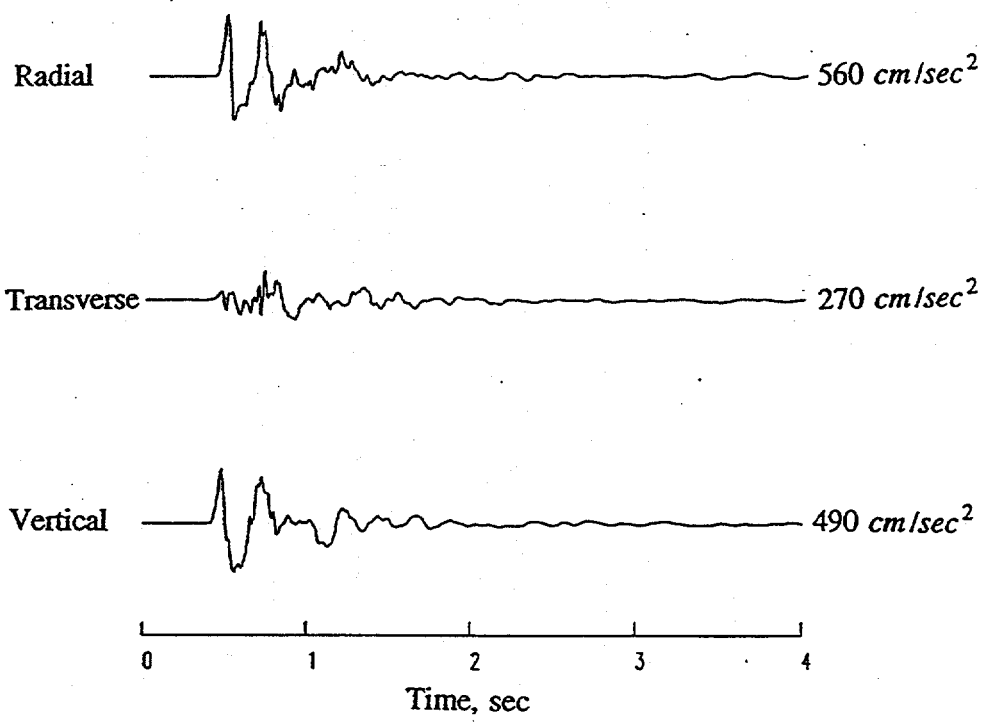
Radial
560 cm/sec²
Transverse
270 cm/sec²
Vertical
490 cm/sec²
0
1
2
3
4
Time, sec

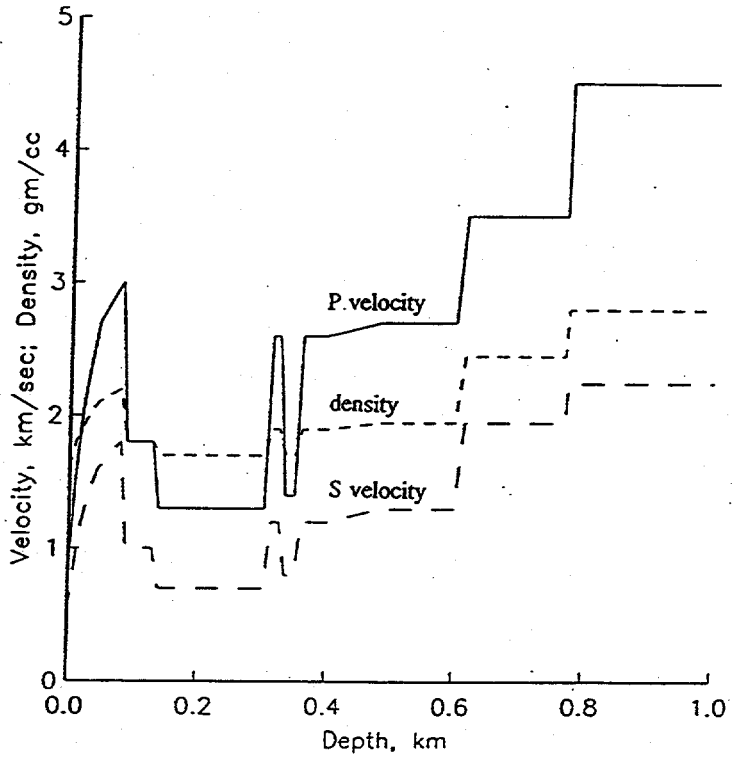
Velocity, km/sec; Density, gm/cc
Depth, km
P velocity
density
S velocity
0
1
2
3
4
5
0.0
0.2
0.4
0.6
0.8
1.0

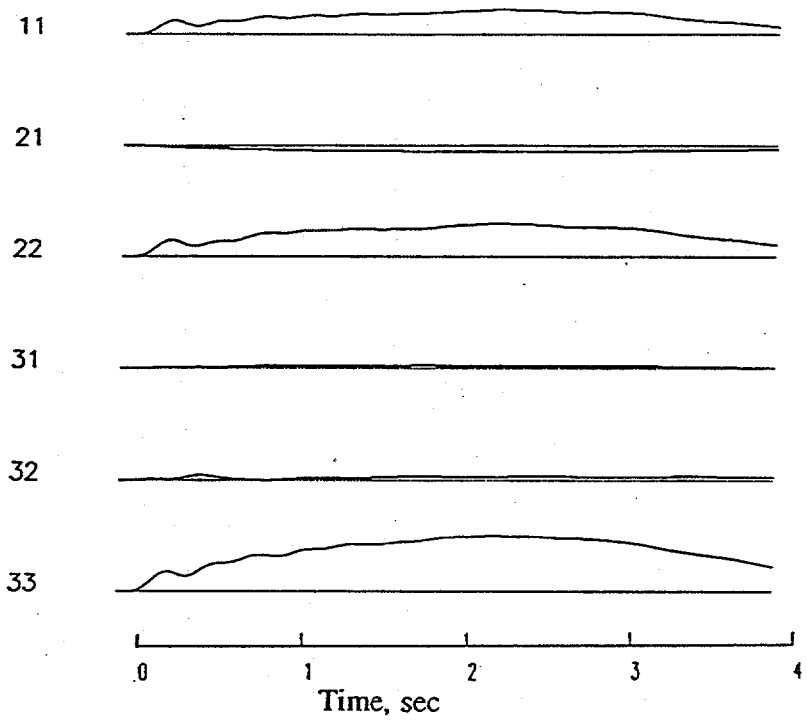
11
21
22
31
32
33
0
1
2
3
4
Time, sec

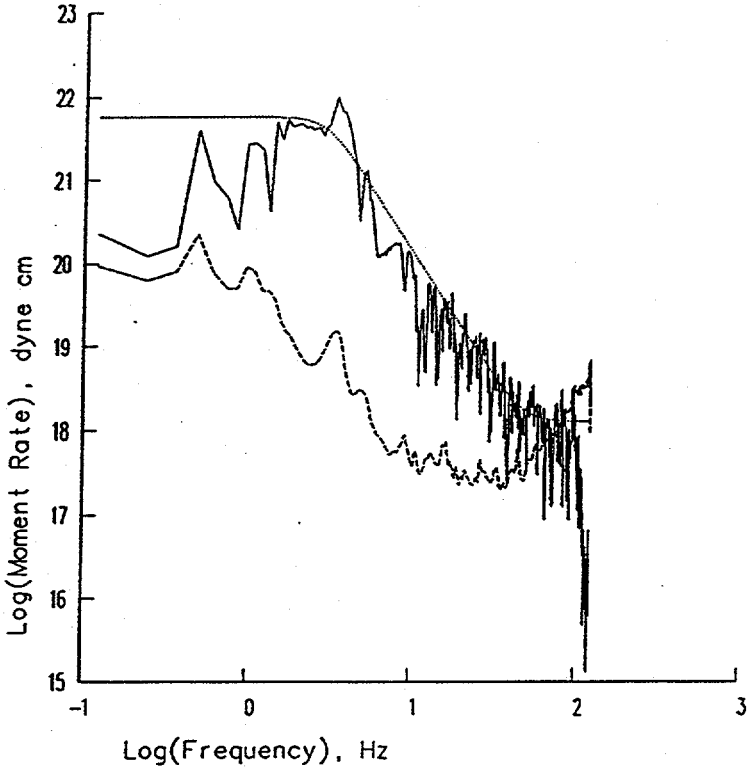
23
22
21
20
19
18
17
16
15
Log(Moment Rate), dyne cm
-1
0
1
2
3
Log(Frequency), Hz

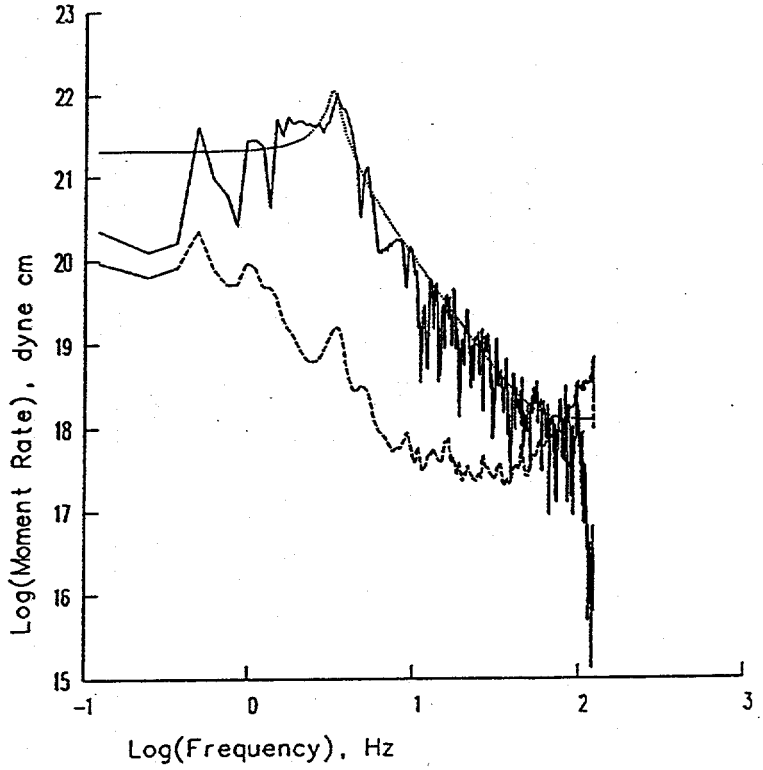
23
22
21
20
19
18
17
16
15
Log(Moment Rate), dyne cm
-1
0
1
2
3
Log(Frequency), Hz